J Fluoresc (2006) 16:287–294
DOI 10.1007/s10895-006-0087-7

ORIGINAL PAPER

Studies on the Interaction of Tricyclazole with β-cyclodextrin and Human Serum Albumin by Spectroscopy

Hua-Xin Zhang · Xing Huang · Ping Mei · Ke-Hua Li · Cheng-Nong Yan

Received: 23 November 2005 / Accepted: 21 February 2006 / Published online: 16 May 2006

Abstract The interaction of tricyclazole (TCZ) with β-cyclodextrin (β-CD) and human serum albumin (HSA) were studied by fluorescence spectrum, UV-visible spectrum and second-order scattering technology. It was shown that TCZ has quite a strong ability to quench the fluorescence launching from HSA by reacting with it and forming a certain kind of new compound. The quenching and the energy transfer mechanisms were discussed, respectively. The binding constants and thermodynamic parameters at four different temperatures, the binding locality, and the binding power were obtained. The conformation of HSA was discussed by synchronous and three-dimensional fluorescence techniques. The inclusion reaction between β-CD and TCZ was explored by scattering method, the inclusion constants and the thermodynamic parameters at 297 K and 311 K were figured out, respectively. The mechanism of inclusion reaction was speculated and linkage among the toxicity of TCZ, the exterior environment and its concentration was attempted to explain on molecule level.

Keywords Tricyclazole · β-cyclodextrin · Human serum albumin · Interaction · Fluorescence · Scattering

Introduction

TCZ (formula: $C_9H_7N_3S$; molecule weight: 189.24), a specific bactericide for rice blast, has a special effect on culm blight of rice and is mainly used for protection in periods of duration. It has been widely applied in agricultural production for its advantage of high absorbency, long period of validity and easy operation, which causes its inevitable residual in rice and environment. Serum albumins are the most abundant proteins in plasma (50%–60% of total amount of plasma proteins) and the main transport proteins. They bind metabolites, endogenous toxins, hormones etc. The detoxifying and regulatory effect of albumin is following: albumin binds the substances and decreases their concentration in a blood because only free fraction of substance is physiologically active [1–3]. Interaction between serum albumins and ligands can provide important information about ligands' storage, transportation, evacuation etc. Thereupon, researches on these have attracted the attention of the biologist, chemist, pharmaceutist and therapist [4–10].

β-CD is composed of seven units of D(+)-glucopyranose units joined by α-1, 4-glycosidic bonds arranged in a truncated cone-shaped structure [11]. As one of the water-soluble cyclic oligosaccharides, it can form inclusion complexes with a large variety of organic and inorganic compounds, which may improve the solubility, stability and bioavailability of guest molecules. As a result, β-CD has been widely applied in food research, organic synthesis, environment protection and especially in the area of pharmacological science [12–17].

The aim of the present work was (1) to study interaction between TCZ and HSA; (2) to study the interaction between TCZ and β-CD. In order to attain these objectives, fluorescence spectroscopy (including emission spectrum, three-dimensional fluorescence spectrum and synchronous fluorescence spectrum) and UV-vis absorption spectroscopy were employed when we carried out detailed investigation of TCZ-HSA association. And the inclusion reaction between

H.-X. Zhang (✉) · X. Huang · P. Mei · K.-H. Li · C.-N. Yan
College of Chemistry and Environmental Engineering, Yangtze University, Jingzhou,
Hubei 434023, People's Republic of China
e-mail: H.X.ZHANG@yeah.net

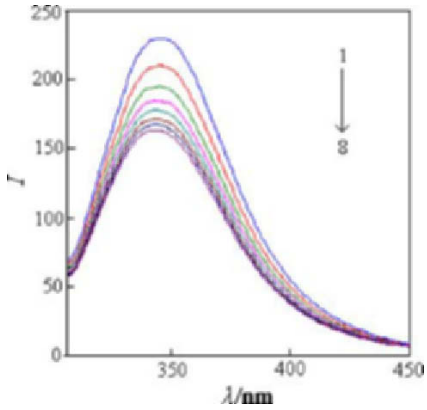

Fig. 1 The fluorescence spectra of HSA in and in no presence of TCZ ($T = 298$ K) $C_{HSA} = 2.000 \times 10^{-5}$ mol L^{-1}; $C_{TCZ}/(10^{-5}$ mol L$^{-1})$, 1–8: 0, 1.585, 3.171, 4.756, 6.341, 7.926, 9.512, 11.10

β-CD and TCZ was studied by second-order scattering technique.

Experimental

Materials

HSA and β-CD were both purchased from Sigma (USA). TCZ was obtained from Sanonda Co., LTD (China). Tris, HCl, NaCl were purchased from Shanghai Chemical Reagent Company (China). TCZ had a purity of no less than 99.5% and all other chemicals were of analytical grade. Stock solutions of HSA (10^{-4} mol L^{-1}), β-CD (0.0300 mol L^{-1}), TCZ (60 mg L^{-1}), NaCl (0.5 mol L^{-1}) and Tris-HCl buffer (0.05 mol L^{-1} Tris, 0.15 mol L^{-1} HCl) of pH 7.40 $\pm$ 0.01 were prepared by directly dissolving the original reagents in water. Water used to prepare solutions was double-distilled.

Apparatus

All fluorescence measurements were carried out on an LS-55 recording spectrophotometer (Perkin-Elmer corporate, America). All ultraviolet-visible spectra were recorded in a UV-1100 spectrophotometer (Beijing, China). The weight measurements were performed with an AY-120 electronic analytic weighing scale (Shimadzu, Japan). All pH measurements were made with a pHS-3 digital pH-meter (± 0.01, Shanghai, China). The specified temperatures were controlled by air conditioners and an SYS-15 digital aqueous thermostat ($\pm 0.01^{\circ}$, Nanjing, China).

Procedure and measurement

The buffer, NaCl, TCZ, β-CD and HSA solutions were added with different ratios into several 10 mL colorimetric tubes, then diluted to 10 mL and stirred well. The solutions were let to stand for 5 min at room temperature, and then react for 30 min at specified temperatures.

In case of the fluorescence spectra of HSA with and without TCZ the excitation wavelength was set at 290 nm and the emission wavelength was set between 275 and 500 nm. In case of fluorescence synchronous scan spectra the initial (excitation) wavelength was set at 160 nm and the wavelength shift $\Delta\lambda$ was equal to 60 nm. In case of the fluorescence spectra of TCZ with and without β-CD the excitation wavelength was set at 230 nm and the emission wavelength was set between 430 and 510 nm. The three-dimensional fluorescence spectrum was performed under the following conditions: the initial excitation wavelength at 200 nm, the emission wavelength between 200 and 490 nm, scanning number 30 and increment 10 nm with other parameters just the same to that of the fluorescence spectra of HSA. In case of absorption spectra scan the slit width was set at 1 nm and the wavelength was set between 200 and 300 nm. The excitation and emission slit widths for all fluorescence spectra were 15 and 2.5 nm and the scanning speed was set at 1200 nm per minute. Samples were contained in 1 cm path length quartz cuvettes.

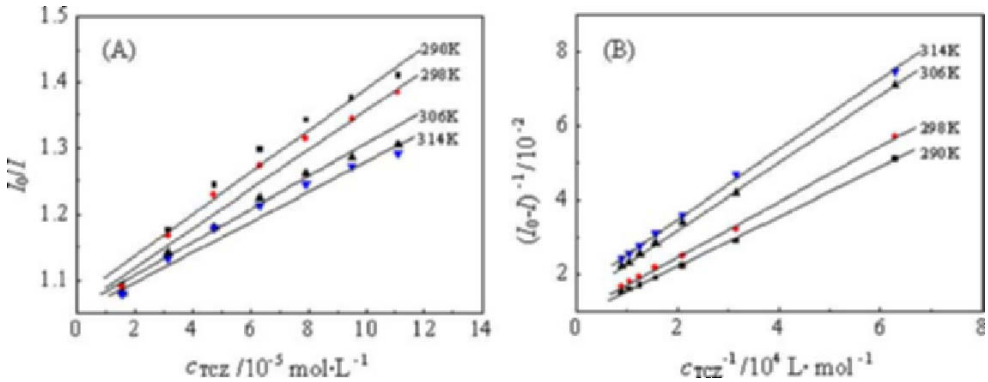

Fig. 2 Stern-volmer curves (A) and lineweaver-burk curves (B) of HSA with certain concentration of TCZ

Table 1 Regression equations and correlation coefficients

Curve	T/K	Regression equations	R
(A)	290	$I_0/I = 1.071 + 3.254 \times 10^3\ C_{TCZ}$	0.9852
	298	$I_0/I = 1.068 + 2.986 \times 10^3\ C_{TCZ}$	0.9864
	306	$I_0/I = 1.062 + 2.355 \times 10^3\ C_{TCZ}$	0.9854
	314	$I_0/I = 1.062 + 2.214 \times 10^3\ C_{TCZ}$	0.9868
(B)	290	$(I_0\text{-}I)^{-1} = 0.008648 + 6.631 \times 10^{-7}\ C_{TCZ}{}^{-1}$	0.9996
	298	$(I_0\text{-}I)^{-1} = 0.009863 + 7.406 \times 10^{-7}\ C_{TCZ}{}^{-1}$	0.9993
	306	$(I_0\text{-}I)^{-1} = 0.01421 + 9.012 \times 10^{-7}\ C_{TCZ}{}^{-1}$	0.9996
	314	$(I_0\text{-}I)^{-1} = 0.01616 + 9.337 \times 10^{-6}\ C_{TCZ}{}^{-1}$	0.9995

Results and discussion

The fluorescence quenching spectra

Fluorescence quenching refers to any process which decreases the fluorescence intensity of a phosphor. A variety of molecular interactions can result in fluorescence quenching, including excited-state reactions, molecular rearrangements, energy transfer, ground-state complex formation, and collisional quenching [18]. The different mechanisms of fluorescence quenching are usually classified as either dynamic quenching or static quenching. Dynamic quenching and static quenching are caused by diffusion and ground-state complex formation, respectively. And they have different dependence on temperature: it is known that higher temperatures result in larger diffusion coefficients, the dynamic quenching constants are expected to increase with increasing temperature. In contrast, increased temperature is likely to result in decreased stability of complexes, and thus lower values of the static quenching constants. Dynamic and static quenching can be distinguished by the absorption spectra before and after two samples interact, as well [19–20].

In this experiment, HSA was phosphor [21] while TCZ acted as the quencher. The fluorescence spectra of HSA and its fluorescence quenching ones by TCZ, were obtained according to procedures mentioned and were shown in Fig. 1.

The fluorescence quenching mechanism

It is apparent, from Fig. 1 that the fluorescence intensity of HSA was decreased regularly with the increase of TCZ concentration, which indicates that there was a certain kind of interaction between TCZ and HSA, and the energy transfer occurred.

In order to conform the quenching mechanism, we analyzed the fluorescence data at different temperatures with the well-known Stern-Volmer equation and Lineweaver-Burk equation, which were commonly used in describing dynamic quenching and static quenching, respectively. Supposing C_P, C_0, I_0, I are the concentration of free fluorescence object, the concentration of all fluorescence object, the fluorescence intensities in the absence and in the presence of quencher, respectively, the equation $C_P/C_0 = I/I_0$ will be reasonable when the formation does not give out fluorescence in a selected wavelength range. Then the Stern-Volmer equation is [19–20, 22]:

$$I_0/I = 1 + K_{SV}[Q] = 1 + K_q\tau_0[Q] \quad (1)$$

where K_{SV} is the Stern-Volmer quenching constant with the unit of L mol^{-1}, [Q] the concentration of the quencher, K_q the quenching rate constant of the biological macromolecule and $K_q = K_{SV}/\tau_0$, τ_0 the average lifetime of the molecule without any quencher and the fluorescence lifetime of the biopolymer is 10^{-8} s.

Lineweaver-Burk equation is [19–20]:

Table 2 Binding constants and thermodynamic parameters derived from K_{LB}

T/K	K_{SV}/L·mol^{-1}	K_q/L·mol^{-1}·s^{-1}	K_{LB}/L·mol^{-1}
290	3.038×10^3	3.038×10^{11}	1.304×10^4
298	2.796×10^3	2.796×10^{11}	1.332×10^4
306	2.218×10^3	2.218×10^{11}	1.577×10^4
314	2.085×10^3	2.085×10^{11}	1.731×10^4

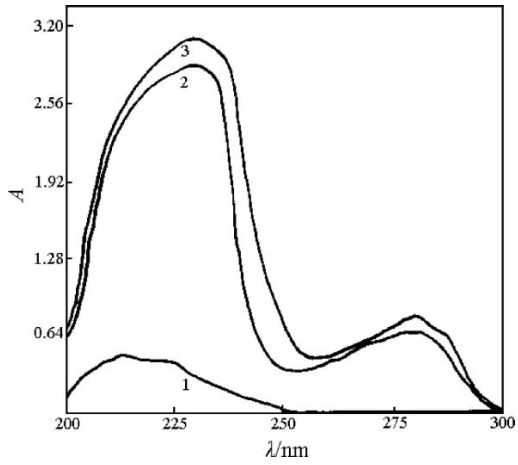

Fig. 3 Absorption spectra of TCZ (1), HSA (2), and TCZ-HSA complex (3) $C_{HSA}/(10^{-5}$ mol L$^{-1})$, 1–3: 0, 2.000, 2.000; $C_{TCZ}/(10^{-5}$ mol L$^{-1})$, 1–3: 2.000, 0, 11.10

Table 3 Thermodynamic parameters derived from K_{LB}

T/K	ΔH^{θ}/kJ·mol^{-1}	ΔS^{θ}/J·K^{-1}	ΔG^{θ}/kJ·mol^{-1}
290	9.071	110.1	−22.85
298		109.4	−23.53
306		110.0	−24.59
314		110.0	−25.48

$$(I_0 - I)^{-1} = (I_0)^{-1} + K_{LB}^{-1} I_0^{-1}[\mathrm{Q}]^{-1} \quad (2)$$

where K_{LB} is the static quenching constant with the unit of L mol^{-1}, which describes the binding efficiency of micromolecules to biological macromolecules at ground state.

Experiments have been done on the fluorescence quenching spectra at four different temperatures and the data have been disposed of according to Stern-Volmer's equation and Lineweaver-Burk equation respectively. These two equation curves are shown in Fig. 2 and their regression equations and correlation coefficients are in Table 1.

Reference has pointed out the maximum scatter collision quenching constant of various quenchers with biopolymer is 2.0×10^{10} L mol^{-1} s^{-1} [22], and it is obvious that the rate constants K_q shown in Table 2 are greater than 2.0×10^{10} L mol^{-1} s^{-1}. From Fig. 2 and Table 1, it can be seen that the curves of Lineweaver-Burk equation have better linear relations. When attention was paid to the value of K_{SV} in Table 2, it could be found that its value became smaller and smaller when the temperature gradually rose. It is exactly the opposite to the definition of dynamic quenching, which can indicate that the quenching was not initiated by collision. Meanwhile, the absorption spectra of HSA-TCZ system (Fig. 3) are clearly different from those of HSA or TCZ alone, which is an obvious evidence that they have formed at least one protein-drug complex with certain new structure. Consequently a conclusion may be safely drawn that the quenching of TCZ to HSA belongs to static quenching

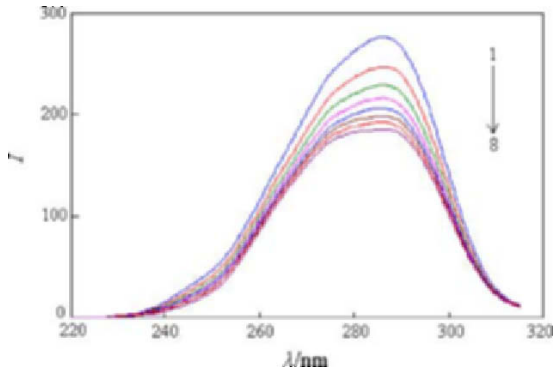

Fig. 4 The effect of TCZ on the synchronous fluorescence spectra of HSA ($\Delta\lambda = 60$ nm) $C_{HSA} = 2.000 \times 10^{-5}$ mol L^{-1}; $C_{TCZ}/(10^{-5}$ mol L$^{-1})$, 1–8: 0, 1.585, 3.171, 4.756, 6.341, 7.926, 9.512, 11.10

with complex formation. And that is why the static binding constants were used when the thermodynamic parameters were calculated.

When the temperature change is not very enormous, the enthalpy change ΔH^{θ} of a system can be regarded as a constant. Under this premise, the thermodynamic parameters deriving from the static binding constants were obtained and showed in Table 3 according to the equation (3)–(5).

$$\Delta G^{\theta} = -RT \ln K^{\theta} \quad (3)$$

$$\ln\left(K_2^{\theta}/K_1^{\theta}\right) = (\Delta H^{\theta}/R) \cdot (1/T_1 - 1/T_2) \quad (4)$$

$$\Delta G^{\theta} = \Delta H^{\theta} - T \cdot \Delta S^{\theta} \quad (5)$$

The effect of TCZ on HSA conformation

Synchronous fluorescence spectroscopy is a common method for evaluating the conformational changes of protein. The synchronous fluorescence spectra of HSA and HSA-TCZ systems were shown in Fig. 4.

Spectroscopy is an ideal tool to observe conformational changes in proteins as it allows non-intrusive measurements of substances in low concentration under physiological conditions. It is advantageous to use intrinsic fluorophores for these investigations in order to avoid complicated labeling with an extrinsic dye. In synchronous spectra, the sensitivity associated with fluorescence is maintained while offering several advantages: spectral simplification, spectral bandwidth reduction and avoiding different perturbing effects. It has been reported that the shift in wavelength of emission maximum λ_{max} corresponds to the changes of polarity around the chromophore molecule [19, 22]. When the wavelength shift ($\Delta\lambda$) between excitation and emission wavelength were stabilized at 60 nm, the synchronous fluorescence gives the characteristic information of tryptophan residues. HSA contains only one tryptophan residue (214-Trp), which makes the absolutely main contribution to the fluorescence intensity of HSA in the wavelength range selected. In Fig. 4, a little, but tangible red shift can be observed, which indicates the Trp-214 residue was placed in a less hydrophobic (or more polar) environment and more exposed to the solvent [20].

Besides, the three-dimensional fluorescence spectra and contour ones were shown in Fig. 5 and Fig. 6.

As known to all, normal fluorescence peaks are usually located in the lower right of the Rayleigh scattering regions. Two typical fluorescence peaks could be easily found in three-dimensional fluorescence spectra. It was obvious that both fluorescence peaks of HSA have been quenched by TCZ, but to different extent (in presence of TCZ, the intensity

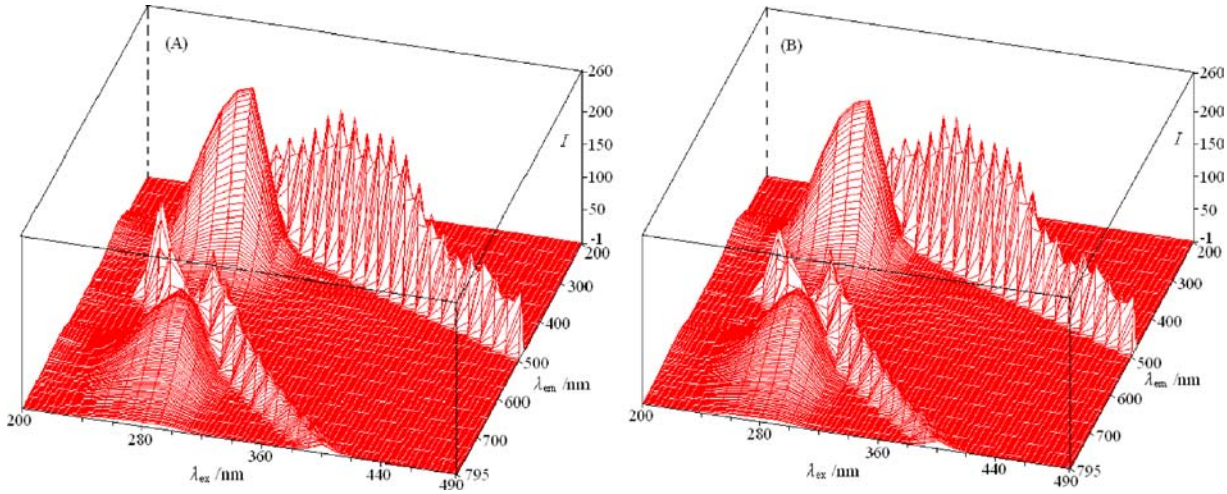

Fig. 5 Three-dimensional fluorescence spectra of HSA (A) and TCZ-HSA complex (B) $C_{HSA}/(10^{-5}$ mol $L^{-1})$, A: 2.000, B: 2.000; $C_{TCZ}/(10^{-5}$ mol $L^{-1})$, A: 0, B: 2.000

ratio of fluorescence peak to second-order one is 2.277:1 while 2.368:1 in absence of it) as shown in Table 4, which indicates that TCZ has complexed with HSA to change its conformation. It is also a substantial evidence that TCZ has obvious poison activity.

Binding force and binding locality

Generally speaking, the force between organic micromolecule and biological macromolecule includes hydrophobic interaction, hydrogen bond, van der Waals force and electrostatic force. Ross etc. summed up the thermodynamic laws for estimating the type of the binding force between organic micro-molecule and biological macromolecule. That is, hydrophobic force may increase ΔH and ΔS of a system, while hydrogen bond and van der Waals power may decrease them, and electrostatic force usually makes $\Delta H \approx 0$ and $\Delta S > 0$ [23]. Based on this rule, the binding power between TCZ and HSA can be regarded as hydrophobic interaction.

In the whole, there was no enhanced fluorescence emission peak of TCZ in fluorescence spectra and three-dimensional spectra, which are the evidence for non-radiation energy transfer. According to Förster's non-radiation energy transfer theory, the energy transfer can occur only when the fluorescence emission spectra of the donor and the absorption spectra of the acceptor have enough overlap and the distance between donor and acceptor is not longer than 7 nm. In detail, it can be described by the following three equations [20, 22]:

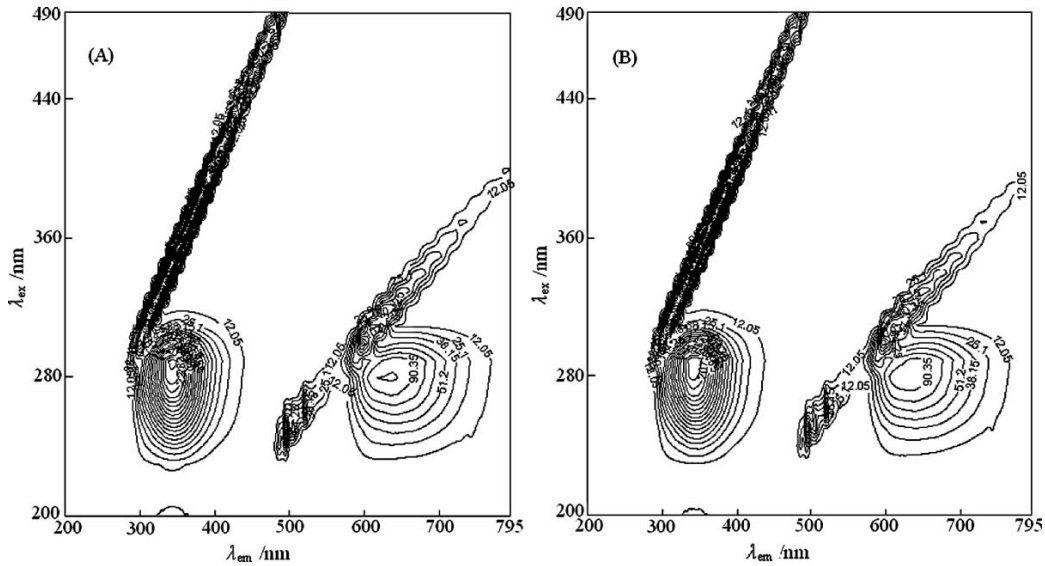

Fig. 6 Contour spectra of HSA (A) and TCZ-HSA complex (B) $C_{HSA}/(10^{-5}$ mol $L^{-1})$, A: 2.000, B: 2.000; $C_{TCZ}/(10^{-5}$ mol $L^{-1})$, A: 0, B: 2.000

Table 4 Three-dimensional fluorescence spectral characteristics of HSA and HSA-TCZ system

Peaks	HSA			HSA-TCZ		
	Peak position ($\lambda_{ex}/\lambda_{em}$)/(nm/nm)	$\Delta\lambda$/(nm)	Intensity I	Peak position ($\lambda_{ex}/\lambda_{em}$)/(nm/nm)	$\Delta\lambda$/(nm)	Intensity I
Rayleigh scattering peaks	280/280→490/490	0	9.902→240.2	280/280→490/490	0	9.035→222.1
Fluorescence peak	290/343	53	250.5	290/342	52	231.6
Second-order scattering peaks	240/480→390/780	λ_{ex}	11.54→156.2	240/480→390/780	λ_{ex}	7.596→117.1
Second-order fluorescence peak	280/633	353	105.8	280/630	350	101.7

$$E = R_0^6/\left(R_0^6 + r^6\right) = 1 - I/I_0 \tag{6}$$

$$R_0 = 8.8 \times 10^{-25}(K^2 \Phi N^{-4} J) \tag{7}$$

$$J = \sum F_D(\lambda)\varepsilon_A(\lambda_0)\lambda^4 \Delta\lambda / \sum F_D(\lambda)\Delta\lambda \tag{8}$$

where E is the efficiency of transfer between the donor and the acceptor, R_0 the critical distance when the efficiency of transfer 50%, r the distance between the acceptor and the donor, K^2 the space factor of orientation, N the refracted index of medium, ϕ the fluorescence quantum yield of the donor, J the effect of the spectral overlap between the emission spectrum of the donor and the absorption spectrum of the acceptor, $F_D(\lambda)$ the corrected fluorescence intensity of the donor in the wavelength range λ_0 to λ, and $\varepsilon_A(\lambda_0)$ the extinction coefficient of the acceptor at λ_0.

The overlap of the absorption spectrum of TCZ and the fluorescence emission spectrum of HSA is shown in Fig. 7. The overlap integral, J, can be evaluated by integrating the spectra in Fig. 7 according to the equation (8). Under our experimental conditions, $K^2 = 2/3$, $N = 1.336$ and $\phi = 0.118$ could be used [19]. Finally, the distance between TCZ and Trp-214 in HSA was calculated to be 2.55 nm.

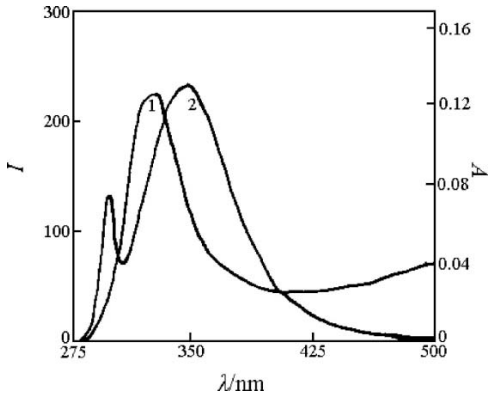

Fig. 7 Overlap of the absorption spectrum of TCZ (1) and the fluorescence emission spectrum of HSA (2) $C_{HSA} = 2.0 \times 10^{-5}$ mol L^{-1}. $C_{TCZ} = 2.0 \times 10^{-5}$ mol L^{-1}

Inclusion reaction of β-CD to TCZ

It is shown that β-CD has enhanced effects on TCZ. An obvious blue shift can be seen for fluorescence peak at 350 nm, which is a significant symbol for inclusion formation. The second-order scattering peak, shown in Fig. 8 with considerable intensity, gets stronger and stronger in presence of increasing concentration of β-CD and good regularity is shown, which can certainly be made use of.

Reference reported a new method for determining inclusion constant between drug and β-CD by non-linear scattering technology. The equation is [24]:

$$1/\Delta I = 1/(rC_G) + 1/(rK_f C_G[CD]) \tag{9}$$

where r is a constant, ΔI equals to I minus I_0, which are the intensity of TCZ with and without β-CD. [CD], C_G, K_f are concentration of β-CD, total concentration of guest molecules, inclusion constant, respectively. When C_G is fixed, $1/\Delta I$ has linear relationship with 1/[CD] (when β-CD is quite excessive, [CD] can be replaced by C_{CD} approximately), and the K_f value can be evaluated by intercept and slope. Fig. 9, by plotting data of $1/\Delta I$ and 1/[β-CD] obtained at different temperatures (297 K, 311 K), shows that the inclusion agree with the new model mentioned above. Regression equations, correlation coefficients, inclusion constants and thermodynamic parameters (supposing enthalpy change ΔH^θ be a con-

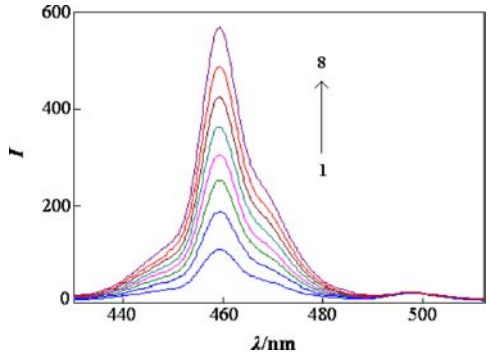

Fig. 8 Effects of β-CD on fluorescence spectra of TCZ $C_{TCZ} = 5.284 \times 10^{-6}$ mol L^{-1}; $C_{\beta-CD}$/(10^{-3} mol L^{-1}), 1→8: 0, 1.500, 3.000, 4.500, 6.000, 7.500, 9.000, 10.50

Table 5 Regression equations, correlation coefficients, inclusion constants and thermodynamic parameters

T/K	Regression equations	R	K_f/L·mol^{-1}	ΔH^θ/KJ·mol^{-1}	ΔS^θ/J·K^{-1}	ΔG^θ/KJ·mol^{-1}
297	$\Delta I^{-1} = 4.199 \times 10^{-4} + 2.100 \times 10^{-5}\, c_{\beta-\mathrm{CD}}{}^{-1}$	0.999 8	20.00	−45.95	129.8	−7.397
311	$\Delta I^{-1} = 1.093 \times 10^{-3} + 1.263 \times 10^{-5}\, c_{\beta-\mathrm{CD}}{}^{-1}$	0.999 7	8.654		129.8	−5.580

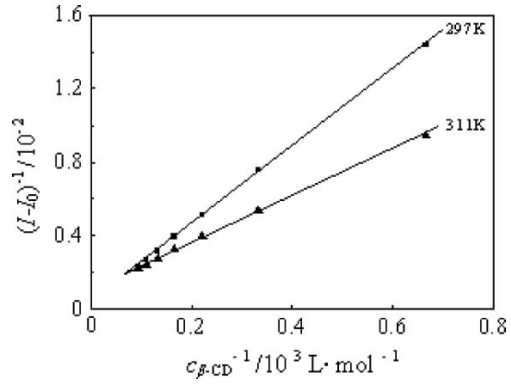

Fig. 9 Plot of $1/\Delta I$ and $1/[\beta\text{-CD}]$

stant as the temperature change is not great) were obtained and showed in Table 5 according to the equation (3)-(5).

Discussion on inclusion reaction mechanism

β-CD, with hydrophobic cavity of inner diameter 7Å, can include TCZ molecule effectively. Fixed by β-CD's inner cavity, the collision frequency of TCZ molecule decreased, the absorption surface expanded. As a result, the quantum yield increased, which appears as an enhanced effect on the luminescence of TCZ. The entropy change ΔS^θ enumerated in Table 5 is 129.8 J K^{-1}, which indicates that this inclusion interaction is spontaneous. The lower values of the inclusion constant with increased temperature may due to decreasing stability of complexes. Further there is no possibility of accommodation of TCZ molecule completely in cavity of β-CD having a length of 7.8Å [25]. So the complex formed is most likely to be the axial inclusion complex with benzene ring of TCZ molecule outside or at least partly outside as shown in Fig. 10. That is why the inclusion constants are not considerable.

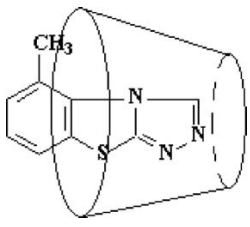

Fig. 10 The most probable molecular structure of β-CD-TCZ inclusion

Conclusions

This paper presents spectroscopic studies on the interaction of TCZ with β-CD and HSA using second-order scattering, fluorescence emission spectrum, UV-visible spectrum, three-dimensional fluorescence spectrum and synchronous fluorescence spectrum. It was shown that the fluorescence of HSA has been quenched for reacting with TCZ and forming a certain kind of new compound. The quenching belonged to static fluorescence quenching, with non-radiation energy transfer happening within single molecule. The binding constant at room temperature was figured out to be 1.332×10^4 L·mol^{-1} and became bigger and bigger when the temperature upgrades. The thermodynamic parameters agree with $\Delta G^\theta < 0$, $\Delta H^\theta > 0$, $\Delta S^\theta > 0$.The binding locality is an area 2.55 nm away from tryptophan residue-214 in HSA and the binding power between them is mainly the hydrophobic interaction. The inclusion constants between β-CD and TCZ at 297 K and 311 K were calculated to be 20.00 and 8.654 L mol^{-1}, respectively. The thermodynamic parameters comply with $\Delta G^\theta < 0$, $\Delta H^\theta < 0$, $\Delta S^\theta > 0$. β-CD has not accommodated TCZ molecule completely in its cavity but it can also mitigate TCZ' toxicity to a certain degree. The next step of our work is to seek for another cyclodextrin which may weak the binding between TCZ and HSA more effectively.

Acknowledgements We gratefully acknowledge financial support of Anton Scholarship provided by Beijing Antonoil Engineering & Technology Co., Ltd.

References

1. Kragh-Hansen U (1990) Structure and ligand binding properties of human serum albumin. Dan. Med. Bull. 37:57–84
2. Cheger SI (1975) Transport Function of Serum Albumin, Buharest, p. 178
3. Sudlow G, Birkett DJ, Wade DN (1975) The characterization of two specific drug binding sites on human serum albumin. Mol. Pharmacol 11:824–832
4. Haque SJ, Poddar MK (1984) Interactions of cannabinoids with bovine serum albumin. Biosci. Rep 4(3):239–243
5. Purohit G, Sakthivel Th, Florence AT (2003) The interaction of cationic dendrons with albumin and their diffusion through cellulose membranes. Int. J. Pharm 254:37–41
6. Borga O, Borga B (1997) Serum protein binding of nonsteroidal anti-inflammatory drugs: A comparative study. J. Pharmacokinet. Biopharm 25:63–77

7. Angelakou A, Valsami G, Macheras P, Koupparis M (1999) A displacement approach for competitive drug-protein binding studies using the potentiometric -anilino-8-naphthalene-sulfonate probe technique. Eur. J. Pharm. Sci 2:123–130
8. Romanini D, Avalle G, Farruggia B, Nerli B, Pico G (1998) Spectroscopy features of the binding of polyene antibiotics to human serum albumin. Chem. Biol. Interact 115(3):247–260
9. Rosso SB, Gonzalez M, Bagatolli LA, Duffard RO, Fidelio GD (1998). Evidence of a strong interaction of 2,4-dichlorophenoxyacetic acid herbicide with human serum albumin. Life Sci 63(26):2343–2351
10. Scatchard G (1949) The attractions of proteins for small molecules and ions Ann. NY Acad. Sci 51:660–672
11. Szejtli J (1988) Cyclodextrine Technology. Kluwer Academic Publishers, Dodrecht, The Netherlands, pp. 143–154
12. Harada A (2001) Cyclodextrin-based molecular machines. Acc Chem Res 34(6):456–464
13. Ikeda H, Nakamura M, Ise N (1996) Fluorescent cyclodextrins for molecule sensing: fluorescent properties, NMR characterization and inclusion phenomena of N-dansylleucine-modified cyclodextrins. J. Am. Chem. Soc 118:10980–10988
14. Szejtli J, Sebesty Gén (1979). Resorption, metabolism and toxicity studies on the peroral application of beta-cyclodextin. Starch 31:385–389
15. Partanen R, Ahro M, Hakala M, Kallio H, Forssell P (2002) Microencapsulation of caraway extract in β-cyclodextrin and modified starches. Eur Food Res Technol 214:242–247
16. Cai WS, Yu YM, Shao XG (2005) Chiral recognition of aromatic compounds by β-cyclodextrin based on bimodal complexation. J. Mol. Model 11:186–193
17. Manabe M, Ochi T, Kawamura H, Katsu-ura H, Shiomi M, Bakshi MS (2005) Volumetric study on the inclusion complex formation of α- and β-cyclodextrin with 1-alkanols at different temperatures. Colloid Polym Sci 283:738–746
18. JR Lakowicz (1999). Principle of Fluorescence Spectroscopy 2nd Ed. Plemum Press, 13
19. Yan CN, Zhang HX, Liu Y, Mei P, Li KH, Tong JQ (2005) Fluorescence spectra of the binding reaction between paraquat and bovine serum albumin. Acta chim. Sinica 63:1727–1732
20. Yan CN, Zhang HX, Liu Y, Mei P (2005) Study on binding reaction between flucytosine and bovine serum albumin. Chin. J. chem 23:1151–1156
21. Stryer L (1968) Fluorescence spectroscopy of proteins. Science 162(853):526–533
22. Vaughan WM, Weber G (1970) Oxygen quenching of pyrenebutyric acid fluorescence in water: a dynamic probe of the microenvironment. Biochemistry 9:464–473
23. Ross DP, Subramanian S (1981) Thermodynamics of protein association reactions: forces contributing to stability. Biochemistry 20:3096–3102
24. Luo HQ, Liu SP, Li NB (2003). New methods for the determination of the inclusion constant between procaine hydrochloride and β-cyclodextrin by resonance nonlinear scattering technology. Acta chim. Sinica 61(3):435–439
25. Muthu Vijayan Enoch IV, Swaminathan M (2004) Inclusion complexation of 2-amino-7-bromofluorene by β-Cyclodextrin: spectra characteristics and the effect of pH. J. Fluorescence 14:751–756